

Bistability and macroscopic quantum coherence in a BEC of ${}^7\text{Li}$.

A. Montana * and F.T. Arecchi †

*Dipartimento di Fisica, Università di Pisa, Via F. Buonarroti 2,
56127 Pisa, Italy

† Dipartimento di Fisica, Università di Firenze
and

INOA (Istituto Nazionale di Ottica Applicata), Largo E. Fermi 6, 50125 Firenze, Italy

(Dated: October 31, 2018)

We consider a Bose-Einstein condensate of ${}^7\text{Li}$ in a situation where the density undergoes a symmetry breaking in real space. This occurs for a suitable number of condensed atoms in a double well-potential, obtained by adding a standing-wave light field to the trap potential. Evidence of bistability results from the solution of the Gross-Pitaevskii equation. By second quantization, we show that the classical bistable situation leads, in fact, to a macroscopic quantum superposition or Schrödinger cat (SC) and evaluate the tunneling rate between the two SC states. The oscillation between the two states is called macroscopic quantum coherence (MQC); we study the effects of losses on MQC.

I. INTRODUCTION

The availability of Bose-Einstein condensates of trapped cold atoms [1, 2, 3, 4] has opened the possibility of a laboratory engineering of quantum states with a large number of atoms [5] (around a thousand for ${}^7\text{Li}$ [4, 6]).

One of the most challenging endeavours of quantum engineering is the evidence of superposition states [so called SC=Schrödinger cat (SC)] whose mutual interference is called macroscopic quantum coherence (MQC). SC have been observed, e.g., for states of a trapped ion [7] and of a microwave field in a high-Q cavity [8].

In this paper we demonstrate the reliable preparation of SC consisting of a Bose-Einstein condensate (BEC) of ${}^7\text{Li}$ atoms that have negative scattering length, trapped in a double-well potential. Realistic calculations have been offered for macroscopic quantum tunneling (MQT) [9, 10]. Indeed, combining the kinetic and potential terms of a harmonic trap with the inter-particle attraction yields a metastable state for $N < N_c$ (N_c = critical population for an attractive BEC). Quantum tunneling from this metastable state towards the collapsed state, which would otherwise be reached for $N > N_c$, has been shown to be feasible.

A BEC of atoms with negative scattering length, trapped in a double well, undergoes a space symmetry breaking beyond a threshold number of atoms N_i , whereby two stable states are formed. This phenomenon has been dealt with theoretically by a two mode approach [11].

We have studied the problem by finding numerically the stationary solutions of the Gross-Pitaevskii (GP) equation discretized over a space lattice, with reference to the ${}^7\text{Li}$ case [12]. Once the stationary solutions have been found, we introduce a quantum two mode model, with the two modes chosen in such a way as to reproduce the stationary solutions of GP. The model shows the feasibility of macroscopic quantum coherence (MQC).

Bistability occurs only for an attractive interatomic

potential (negative scattering length). Two proposals for reaching SC in a BEC with repulsive atoms have been put forward [13, 14]. They both require a Raman coupling between two different components; Both the papers consider copropagating light beams. In Ref. [13], MQC is shown to require values of the scattering length between atoms of different magnetic number substantially larger than the scattering length between atoms of equal magnetic number. This requirement is too strong, since no experimental technique is today accessible to provide such a difference; furthermore, if such a difference could be achieved, outstanding symmetry-breaking effects would occur [15]. Reference [14] introduces a time-dependent evolution, so that SC is reached over a time of the order of 1 sec. However, no clear-cut experimental test is offered to discriminate between SC and a statistical mixture of two separate states.

II. BISTABILITY AND SYMMETRY BREAKING

We refer to a condensate of ${}^7\text{Li}$ atoms trapped in a double-well potential. A suitable model for it is given by

$$V(\vec{x}) = \frac{1}{2}m \left[\omega_{\parallel}^2 x_1^2 + \omega_{\perp}^2 (x_2^2 + x_3^2) \right] + A \cdot \cos \left(2\pi \frac{x_1}{\sigma} \right) \quad (1)$$

The quadratic part is due to the interaction of the atoms with the magnetic field of the trap. According to laboratory implementations [4] we choose $\omega_{\parallel} = 2\pi \times 130\text{s}^{-1}$ and $\omega_{\perp} = 2\pi \times 150\text{s}^{-1}$. The additional term is generated by two opposite laser beams in a standing wave configuration. A suitable choice of the standing-wave parameters yields a double well-potential. Taking into account the interatomic interaction, the atomic system is described by a macroscopic wave function ψ that satisfies the GP equation

$$i\hbar \frac{\partial \psi}{\partial t} = -\frac{\hbar^2}{2m} \nabla^2 \psi + V\psi + g|\psi|^2 \psi \equiv (H + g|\psi|^2)\psi, \quad (2)$$

with $H = -\hbar^2/(2m)\nabla^2 + V$. Here, $m \simeq 7a.u.$ is the mass of the lithium atom, and $g = (4\pi\hbar^2/m)a_s$, where a_s is the s-wave scattering length for ${}^7\text{Li}$, $a_s \simeq -1.45\text{nm}$. For a small number of atoms the GP nonlinearity can be neglected and Eq. (2) reduces to an ordinary Schrödinger equation. In such a case and for a sufficiently high barrier, the lowest energy level is described by a two-peak wave function symmetric with respect to inversion of the space axes, once the coordinate origin coincides with the trap center (Fig. 1, dashed-dot line).

Figure 1 reports the spatial distribution of the ground state of Eq. (2) for different numbers of trapped atoms; we have used a numerical method that consists in solving GP on a discrete space lattice and evaluating the lowest energy state. The barrier is specified by the two parameters $A_n \equiv A/\hbar = 2650\text{s}^{-1}$ and $\sigma = 5\mu\text{m}$ (see Eq. (1)). As shown in the figure, for $N = 450$ the distribution is symmetric; instead for $N = 500$ the nonlinear term is sufficient to destabilize the symmetric state, giving rise to two asymmetric stable states. For $N = 600$ one well is almost empty. As we increase the number of atoms, the nonlinearity plays a relevant role. By a self-consistent argument we realize that the symmetric wave function becomes unstable and we can have two new minimal energy states with distribution no longer symmetric for inversion (symmetry breaking). Indeed, let us assume a distribution as in Fig. 1 (dashed or solid line); then the effective potential for such a distribution, due to the sum of the external potential with $g|\psi|^2$ is an asymmetric double well with the lower minimum corresponding to the higher population peak. For a sufficiently high nonlinear term the potential imbalance stabilizes the asymmetric distribution as in Fig. 1.

We confirm the numerical calculation by the following analytic model. Let ψ_a be the equilibrium symmetrical wave function (either stable or unstable), and ψ_b be a suitable antisymmetrical wave function such that the weighted sum of the two wave functions lowers either one of the two peaks. In the two-dimensional space of these wave functions, any other one can be expressed as

$$\psi(\vec{x}) = a\psi_a(\vec{x}) + b\psi_b(\vec{x}). \quad (3)$$

Without loss of generality we can choose ψ_a and ψ_b as real functions and thus consider real values for a and b . As we take $\int \psi_a^2 d^3x = \int \psi_b^2 d^3x = 1$, it follows that $a^2 + b^2 = \int \psi^2 d^3x \equiv M(a, b)$, where $M(a, b)$, the total number of atoms in the condensate, depends upon a and b . The energy is then given by

$$\mathcal{H} = a^2 H_{aa} + b^2 H_{bb} + \frac{1}{2}(a^4 I_{aa} + b^4 I_{bb}) + 3a^2 b^2 I_{ab} \quad (4)$$

where

$$H_{aa} = \int \psi_a^* H \psi_a d^3x, \quad H_{bb} = \int \psi_b^* H \psi_b d^3x,$$

$$I_{aa} = g \int \psi_a^4 d^3x, \quad I_{bb} = g \int \psi_b^4 d^3x,$$

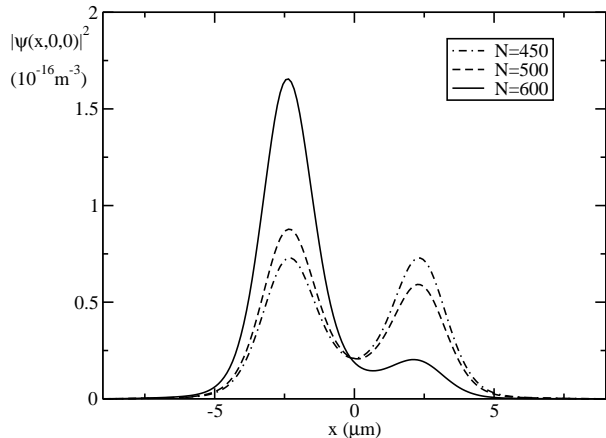


FIG. 1: Density distribution of the lithium BEC in real space for $N = 450$ (dash-dotted line), $N = 500$ (dashed line), and $N = 600$ (solid line) with $A_n \equiv A/\hbar = 2650\text{s}^{-1}$ and $\sigma = 5\mu\text{m}$.

$$I_{ab} = g \int \psi_a^2 \psi_b^2 d^3x.$$

We look for the minimal of energy with the constraint of a fixed number N of condensed atoms. These constrained minima satisfy the relations

$$\frac{\partial(\mathcal{H} - \mu M)}{\partial a} = \frac{\partial(\mathcal{H} - \mu M)}{\partial b} = 0, \quad (5)$$

where μ is a Lagrange multiplier. We thus solve for a and b , with the condition $N = a^2 + b^2$. The solutions $a = 0$ and $b = 0$ correspond, respectively, to the antisymmetric function and the symmetric one. The other solutions, for both a and b nonzero, yield a^2, b^2 values as functions of μ . Using the constraint of fixed N , we eliminate μ and find

$$a^2 = \frac{H_{aa} - H_{bb} + N(3I_{ab} - I_{bb})}{6I_{ab} - I_{aa} - I_{bb}} \quad (6)$$

$$b^2 = \frac{H_{bb} - H_{aa} + N(3I_{ab} - I_{aa})}{6I_{ab} - I_{aa} - I_{bb}} \quad (7)$$

Since g is negative, the denominator is always negative. Indeed, ψ_a^2 and ψ_b^2 are almost equal at each point x . For low N , the dominant terms in the numerators have opposite sign, thus one of the two squares has to be negative, which means that there is no solution with asymmetric wave function. On the other hand, for sufficiently large N , the second term in the numerator of the two equations can compensate for the positive one, since the quantities $3I_{ab} - I_{aa}$, $3I_{ab} - I_{bb}$ are always negative. Thus, we have proved that two asymmetrical steady states exist beyond a threshold value of N .

In order to prove that the two states are stable, it is sufficient to show that the symmetrical state becomes

unstable above threshold, that is,

$$\left. \frac{d^2 \mathcal{H}}{db^2} \right|_{b=0} \leq 0 \quad (8)$$

where we have $a^2 = N - b^2$. It is easily found that

$$\left. \frac{d^2 \mathcal{H}}{db^2} \right|_{b=0} = 2(H_{bb} - H_{aa}) + 2N(3I_{ab} - I_{aa}) \quad (9)$$

Going back to Eq. (7), the two stationary asymmetrical states occur when the numerator changes sign. In fact, the numerator is the right side of Eq. (9), hence, at the critical point the symmetrical state becomes unstable.

One can easily evaluate the threshold value N_i of N for which this symmetry breaking occurs.

III. MACROSCOPIC QUANTUM COHERENCE

In such a bistable situation the energy displays two minima of equal value in the infinite-dimensional phase space. From a classical point of view, as the system is in its lowest energy state, the condensate is localized in either one of the two minima, where it will remain in the absence of thermal noise once we keep the atom number constant. Since, however, the condensate is a mesoscopic system, quantum fluctuations play a relevant role. This can be shown by second quantization of the field, replacing the c-number macroscopic wave function by field operators.

Quantum fluctuations allow the passage from one to the other stable state without thermal activation, by pure quantum tunneling. Furthermore, due to the coherent nature of the process, we expect coherent oscillations between the two wells, that is, MQC. We now evaluate the tunneling rate as a function of the system parameters showing the feasibility of MQC.

The most natural way of evaluating the tunneling rate consists in finding the two lowest eigenvalues of the Hamiltonian and taking their difference. Indeed, the sum and difference of the corresponding states are respectively the alive and dead states of SC, and the transition time is half the period corresponding to the frequency difference.

The problem is simplified by reducing it to two degrees of freedom by the expansion of Eq.(3).

We select the basis functions ψ_a and ψ_b as follows. Calling $\psi_0(\vec{x})$ the minimal-energy wave function of the GP problem (see e.g. Fig. 1), we take for ψ_a and ψ_b , respectively, the symmetric and antisymmetric sums $\psi_0(\vec{x}) \pm \psi_0(-\vec{x})$. Expansion (3) with these ψ_a and ψ_b includes the original functions $\psi_0(\vec{x})$ and $\psi_0(-\vec{x})$ for suitable values of a and b . Furthermore, it simplifies the form of the Hamiltonian, as we see right now [16].

In second quantization, a and b in Eq. (3) become the operators \hat{a} and \hat{b} , obeying Bose commutation rules with

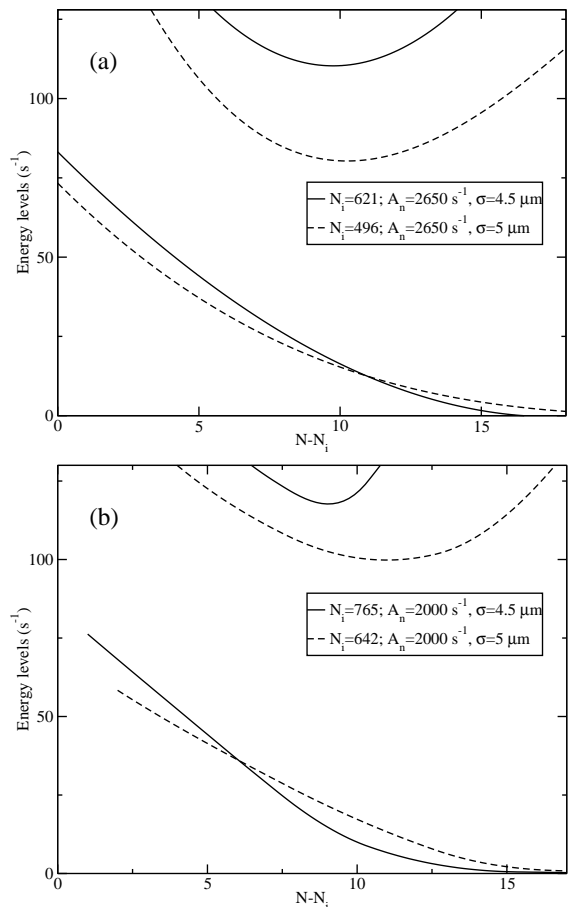


FIG. 2: First two excited energy levels versus the number $N - N_i$ of atoms above the threshold N_i . Within each figure we keep the laser amplitude fixed and just vary the pitch of the potential lattice; (a) corresponds to $A_n \equiv A/\hbar = 2650s^{-1}$ and (b) corresponds to $A_n = 2000s^{-1}$.

their conjugates \hat{a}^\dagger , \hat{b}^\dagger . Exploiting the operator version of Eq. (3) and its adjoint, the Hamiltonian becomes

$$\mathcal{H} = \hat{a}^\dagger \hat{a} H_{aa} + \hat{b}^\dagger \hat{b} H_{bb} + \frac{1}{2}(\hat{a}^{\dagger 2} \hat{a}^2 I_{aa} + \hat{b}^{\dagger 2} \hat{b}^2 I_{bb}) + \quad (10)$$

$$\left(\frac{1}{2} \hat{a}^{\dagger 2} \hat{b}^2 + \frac{1}{2} \hat{b}^{\dagger 2} \hat{a}^2 + 2\hat{a}^\dagger \hat{b}^\dagger \hat{a} \hat{b} \right) I_{ab}$$

where the coefficients H_{aa} , H_{bb} , I_{aa} , I_{bb} and I_{ab} are the same as in Eq. (4).

We consider the basis of eigenvectors of the number operators

$$|0, N\rangle, |1, N-1\rangle, \dots, |N, 0\rangle \quad (11)$$

where $\hat{a}^\dagger \hat{a} |k, m\rangle = k |k, m\rangle$ and $\hat{b}^\dagger \hat{b} |k, m\rangle = m |k, m\rangle$. Let us call

$$H_{l,k} = \langle l, N-l | \mathcal{H} |k, N-k\rangle \quad (12)$$

the generic matrix element of the Hamiltonian on the above basis. We evaluate the eigenvalues of this matrix.

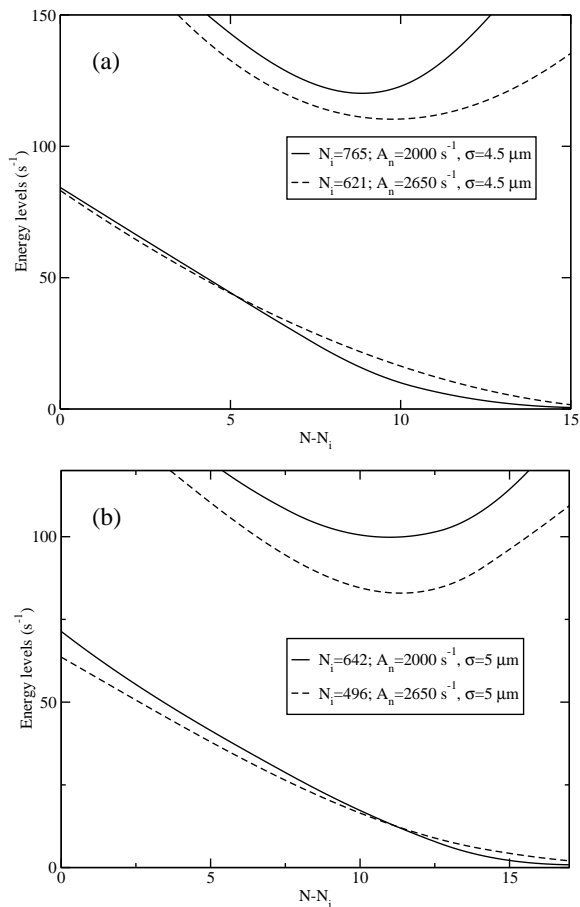


FIG. 3: Same as with Fig. 2, but with fixed σ , respectively (a) $\sigma = 4.5\mu m$ and (b) $\sigma = 5\mu m$.

We have considered two different wavelengths and two amplitude values of the applied field.

In Fig. 2 we report on the first two excited energy levels versus the number of condensed atoms beyond the threshold value. In such figure we keep constant the barrier height and just vary the barrier width. Notice that for increasing σ the maximum tunneling frequency reduces, but the slope at which it reduces for increasing $N - N_i$ is less steep.

In Fig. 3 we keep fixed the barrier width and change its height. Here too the maximum frequency decreases for increased heights, but again as in Fig. 2, the slope decreases for increasing $N - N_i$.

In Fig. 4 we reduce the threshold for BEC breaking by increasing ω_{\perp} . Precisely, we report on the first two excited states for $\omega_{\perp} = 2\pi \times 600s^{-1}$, $A_n = 2000s^{-1}$ and $\sigma = 5\mu m$. The threshold value is $N_i \simeq 190$.

In the number representation there is no explicit evidence of a SC as a two-peak distribution (see Fig. 5). We look for a suitable observable, whose probability distribution provides such an evidence. We take the first component of the barycenter coordinate $x_c = (1/N) \int x_1 |\psi|^2 d^3x$ as the appropriate variable since the corresponding classical states [minima of the Hamilto-

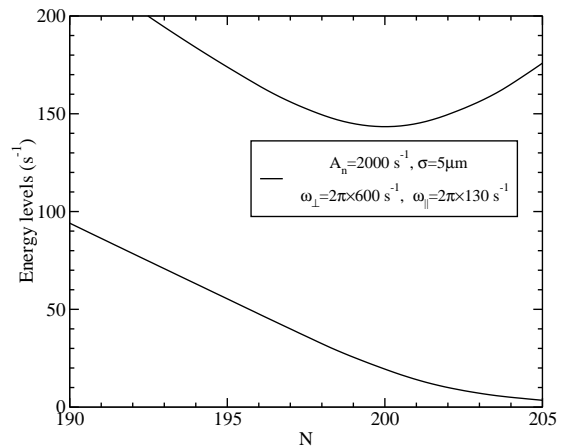


FIG. 4: First two excited energy levels versus the number of atoms N . The system parameters are $\omega_{\perp} = 2\pi \times 600s^{-1}$, $\omega_{\parallel} = 2\pi \times 130s^{-1}$, $A_n \equiv A/\hbar = 2000s^{-1}$ and $\sigma = 5\mu m$.

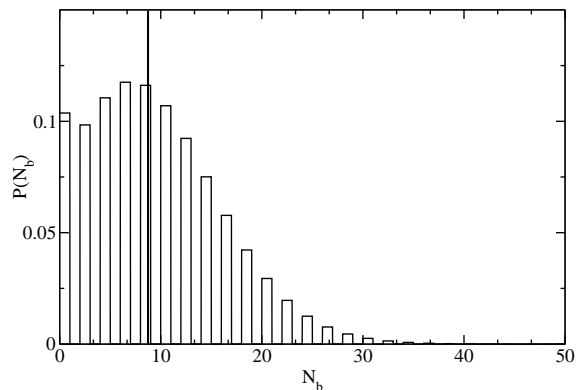


FIG. 5: Probability distribution of the population in the ground state as a function of the number of atoms in mode 'b'. $A = 2000s^{-1}$, $\sigma = 5\mu m$ and $N = 655$.

nian (4)] have separated barycenters. It is associated with the operator

$$\hat{x}_c = \frac{1}{N} \int x_1 \psi_a(\vec{x}) \psi_b(\vec{x}) d^3x (\hat{a}^\dagger \hat{b} + \hat{a} \hat{b}^\dagger) \quad (13)$$

Besides a c-number factor, the observable is thus $\hat{M} = \hat{a}^\dagger \hat{b} + \hat{a} \hat{b}^\dagger$. The associated probability density is $P(m) = |\langle m | \phi_0 \rangle|^2$, where $|\phi_0 \rangle$ is the ground state of Hamiltonian (10) and $|m \rangle$ is the eigenstate of \hat{M} with eigenvalue m . Notice that once the number of atoms is fixed the eigenvectors are not degenerate.

Since we know the components of $|\phi_0 \rangle$ on the number basis we must express $|m \rangle$ with respect to that basis, that is,

$$|m \rangle = \sum_k c_k^m |k, N - k \rangle. \quad (14)$$

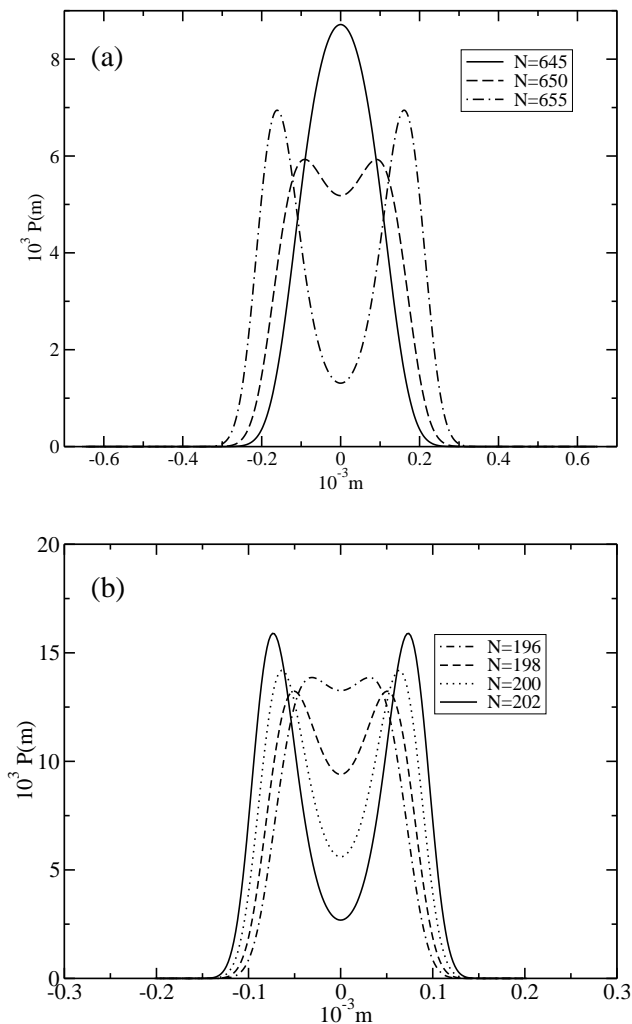


FIG. 6: Probability distribution of the "barycenter" indicator for the lithium BEC, for different N values and for a standing wave with $A_n = 2000s^{-1}$ and $\sigma = 5\mu m$; (a) $\omega_{\perp} = 2\pi \times 150s^{-1}$ and (b) $\omega_{\perp} = 2\pi \times 600s^{-1}$.

Applying the operator \hat{M} to the above ket we have

$$m|m\rangle = \sum_k c_k^m (\hat{a}^\dagger \hat{b} + \hat{a} \hat{b}^\dagger) |k, N-k\rangle. \quad (15)$$

Projecting on $\langle l, N-l|$ the above ket it follows that

$$\sum_k M_{l,k} c_k^m = m c_l^m, \quad (16)$$

where

$$M_{l,k} = \langle l, N-l | \hat{M} | k, N-k \rangle. \quad (17)$$

Since $M_{l,k}$ are known, solving the eigenvector equation (16) we can evaluate the coefficients c_k^m and hence $P(m)$.

The two-peak distribution $P(m)$ is plotted in Fig. 6(a) for different N values and for $A/\hbar = 2000s^{-1}$, $\sigma = 5\mu m$.

The same distributions, but for $\omega_{\perp} = 2\pi \times 600s^{-1}$, are given in Fig. 6(b).

Experimentally, evidence of SC against a trivial statistical mixture is obtainable by setting the system at the above parameter values and observing the coherent oscillation between the two energy minima by a measurement not destroying the coherence (e.g., a phase contrast technique). The condensate can be prepared in the ground state, because the system condensates naturally in this state. Then one measures the condensate barycenter by the above noninvasive technique at the initial time. This measurement collapses the distribution $P(m)$ onto one peak. If the energy transfer of the measurement is not too large, we expect that only the first excited state is populated and hence we have the superposition of $\phi_0(m)$ and $\phi_1(m)$ [see Fig. 7(a)]. At the following times the distribution oscillates between the two peaks. The symmetry of Hamiltonian (10) with respect to the transformation $\hat{a} \rightarrow -\hat{a}$ shows that $\phi_0(m)$ and $\phi_1(m)$ are symmetric or antisymmetric; by a suitable choice of the phase, both ϕ_0 and ϕ_1 can be real functions. We consider a state preparation such that at $t = 0$ the state $\phi_0(m) + \phi_1(m)$ has only one probability peak [see Fig. 7(a), dashed line]. After a quarter period corresponding to the frequency separation ω_f between ground and first excited states, the superposition will be $\phi_0(m) - i\phi_1(m)$ and the corresponding probability is the two-peak aspect (solid line),

$$Q(m, t = \pi/\omega_f) = \phi_0(m)^2 + \phi_1(m)^2. \quad (18)$$

At time $t = \pi/\omega_f$ the only peak is that missing at time $t = 0$, thus there is a coherent oscillation between the two states. Detecting such an oscillation would provide evidence of an SC at an intermediate time when both peaks are present.

The intermediate distribution, given by Eq. (18), may display two peaks even when the ground state has only one [see Fig. 7(b)]. This occurs because the distribution $\phi_1(m)^2$ has always two peaks.

Notice that if we had N loosely coupled or independent atoms (Ng sufficiently low or even zero) the superposition of ground and first excited state would have a single peak, oscillating as a coherent state inside a harmonic potential. This would by no means be a SC. On the contrary, we have shown that for Ng sufficiently high, we have a two peak distribution with the two partial barycenters at nearly constant positions. During the evolution, the two peak amplitudes oscillate, that is, the probability to find the system in either state oscillates.

In conclusion, we have found that the oscillation frequency between the two states of the SC is $\omega_f \sim 50s^{-1}$ [see Fig. 2(a) for $N - N_i \sim 5$]. In order to neglect thermal activation, the system should be cooled at a temperature of around $1nK$. To cool at $1nK$ is within the reach of present technologies, even though such a low temperature has not yet been reported. On the other hand, the collective degrees of freedom for which there is quantum coherence may be weakly coupled with the other modes of the condensate, which act as a thermal bath. Hence,

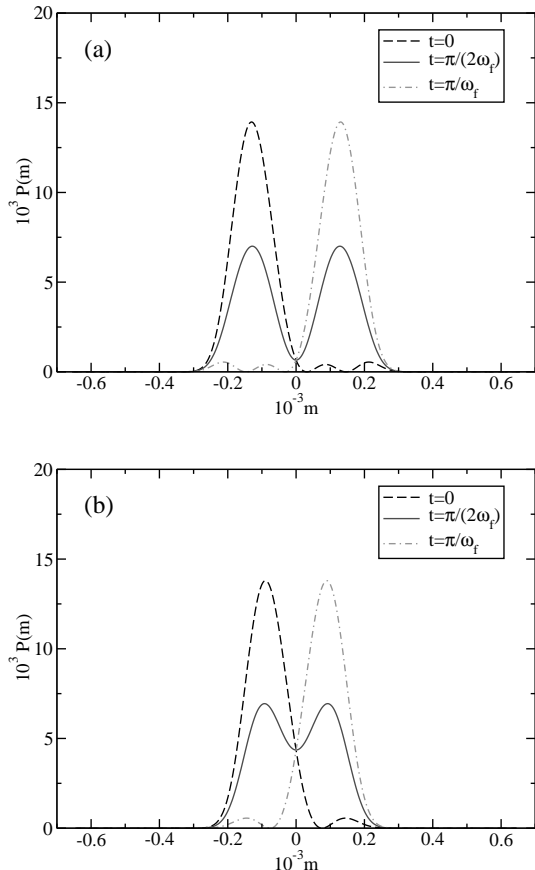


FIG. 7: Time evolution of the probability distribution. ω_f is the tunneling frequency. The parameters of the standby wave are as in Fig. 6(a); (a) number of atoms $N = 655$ and (b) $N = 645$, for which the ground state does not display two separate peaks [see solid line of Fig. 6(a)].

in such a case it might not be necessary to cool at $1nK$ the whole condensate, but just the involved degrees of freedom.

IV. LOSSES AND OBSERVABILITY OF MQC

Besides the finite temperatures effects, we must also account for atom losses from the condensate.

The entanglement between condensate and lost atoms will imply a decoherence of the superposition. Near the threshold for symmetry breaking, the two macroscopic wave functions corresponding to the energy minima of the classical system are almost coincident (see Fig. 1, for $N = 500$), thus the loss of one or a few atoms does not allow us yet to discriminate between the two alternatives, and thus decoherence effects are almost negligible.

We perform a simple calculation of the decoherence effect due to atom loss for the condensate. In the Hartree-Fock approximation all the atoms are in the same state, given by the GP wave function. Hence, if $\psi_0(\vec{x})$ is one

of the two asymmetrical states with minimal energy, the wavefunction for the whole system of N atoms is given by

$$\psi_l(\vec{x}_1, \vec{x}_2, \dots, \vec{x}_N) = \prod_{i=1}^N \psi_0(\vec{x}_i). \quad (19)$$

But the GP yields another minimum $\psi_0(-\vec{x})$, for which the overall wave function is given by

$$\psi_r(\vec{x}_1, \vec{x}_2, \dots, \vec{x}_N) = \prod_{i=1}^N \psi_0(-\vec{x}_i). \quad (20)$$

The coherent superposition of the two alternatives is given by

$$\psi_s = K(\psi_l + \psi_r) \quad (21)$$

where K is a normalization factor. If $\psi_{l,r}$ are orthogonal then $K = \frac{1}{\sqrt{2}}$.

The density operator is

$$\hat{\rho} = \frac{1}{2} (|\psi_l\rangle + |\psi_r\rangle)(\langle\psi_l| + \langle\psi_r|) \quad (22)$$

The coherence between the two alternatives is given by

$$C = 2Tr[|\psi_l\rangle\langle\psi_r|\hat{\rho}] = 1. \quad (23)$$

If we assume that the atoms escaping the condensate transfer a negligible energy to the trapped atoms, then the residual coherence after the loss of M atoms is

$$\tilde{C} = 2Tr[|\tilde{\psi}_l\rangle\langle\tilde{\psi}_r|\hat{\rho}], \quad (24)$$

where the vectors $|\tilde{\psi}_{l,r}\rangle$ refer to the $N - M$ atoms still in the condensate. The functions $\psi_{l,r}$ can be written as

$$\psi_{l,r} = \tilde{\psi}_{l,r} \prod_{i=1}^M \psi_0(\pm\vec{x}_i), \quad (25)$$

where $i = 1, 2, \dots, M$ are the lost atoms. We rewrite $\hat{\rho}$ by using this expansion, and find, provided that $\langle\tilde{\psi}_l|\tilde{\psi}_r\rangle = 0$,

$$\tilde{C} = \left(\int d^3x \psi_0(\vec{x})\psi_0(-\vec{x}) \right)^M \equiv (I_o)^M. \quad (26)$$

Let us call $\epsilon = 1 - I_o$. If $\epsilon \ll 1$ then the coherence is given by

$$\tilde{C} \simeq e^{-\epsilon M}. \quad (27)$$

The quantity $N_d = 1/\epsilon$ provides the number of atoms that must be lost in order to reduce the coherence by $1/e$. Figure 8 shows how N_d scales with the total number of atoms N for $A = 2000s^{-1}$ and $\sigma = 5\mu m$.

Notice that near the threshold value ($N = 643$) N_d is rather large, and hence, coherence is more robust with respect to atom losses. Far threshold N_d has a weak dependence on N .

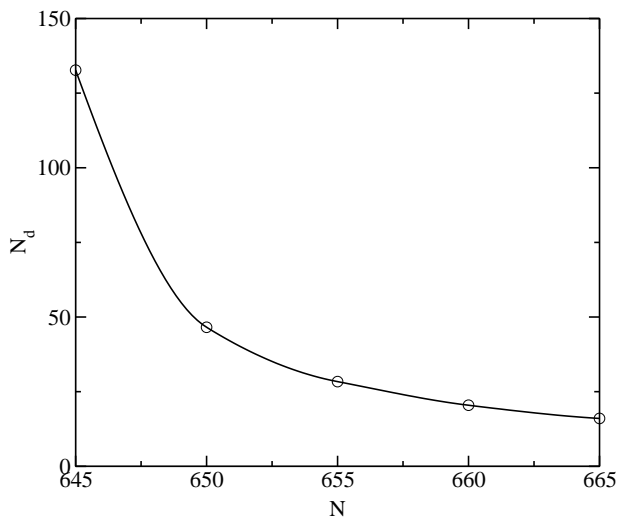


FIG. 8: Number N_d of lost atoms for which the coherence decays by $1/e$ versus the total number of atoms, for $A_n \equiv A/\hbar = 2000s^{-1}$ and $\sigma = 5\mu m$.

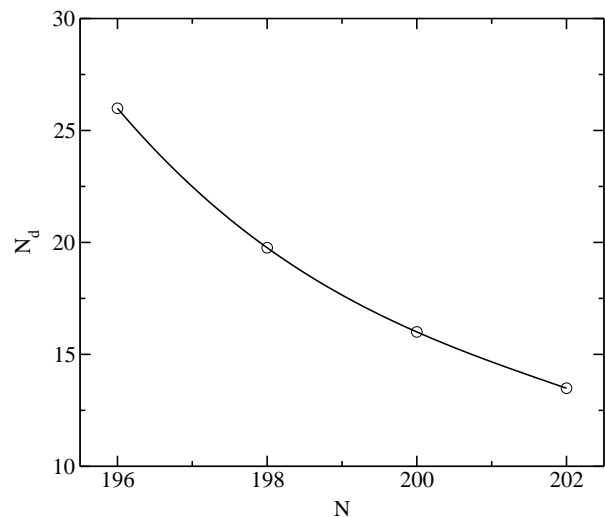


FIG. 10: Number N_d of lost atoms for which the coherence decays by $1/e$ versus the total number of atoms, for the parameters of Fig. 4.

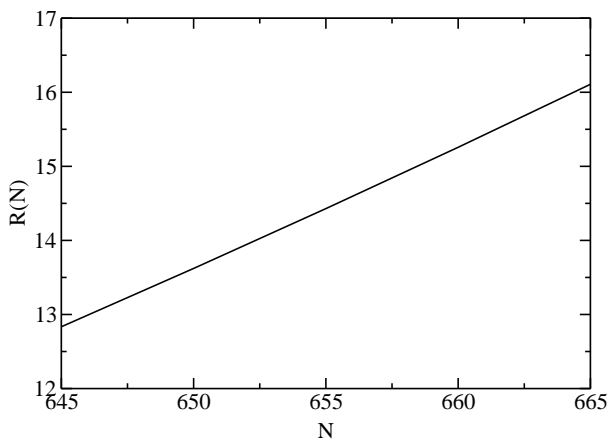


FIG. 9: $R(N)$ for $A_n \equiv A/\hbar = 2000s^{-1}$ and $\sigma = 5\mu m$.

We now evaluate the loss rate of the condensate. The relevant processes are two-body inelastic and three-body collisional decays. The total loss rate of the two decays are [17]

$$R(N) = \alpha N^2 \int d^3r |\psi_0(r)|^4 + LN^3 \int d^3r |\psi_0(\vec{x})|^6 \quad (28)$$

where α is the two-body dipolar loss rate coefficient and L is the three-body recombination loss rate coefficient. We use the following values: $\alpha = 1.2 \times 10^{-14} cm^3 s^{-1}$ [17], $L = 2.6 \times 10^{-28} cm^6 s^{-1}$ [18].

We report in Fig. 9 $R(N)$ for $A = 2000s^{-1}$ and $\sigma = 5\mu m$. From Figs. 2(b), 8, and 9 we can infer that near threshold atom losses have a small effect on coherence.

For instance, for $N = 650$ the tunneling rate is about

$25s^{-1}$ [see Figs. 2(b) and 3(b)], thus the number of atoms lost during an oscillation period ($\sim 0.25s^{-1}$) is around 3.5 (see Fig. 9); but Fig. 8 shows that such a loss is negligible for coherence. For $N = 655$ the tunneling rate is about $10s^{-1}$, thus the number of atoms lost during an oscillation period is about 9, still below $N_d \simeq 30$.

Besides decoherence, the atom loss yields a shift in the tunneling frequencies. As shown in Figs. 2-3, the frequencies vary a lot as we reduce the number of condensed atoms. For $N = 650$ the lost atoms are around 3.5 during an oscillation period, thus the oscillation frequency changes by $\sim 30\%$.

In order to reduce the effect of losses we lower the threshold value by increasing the frequency ω_{\perp} . In Figs. 10 and 11 we report on N_d and $R(N)$ for $\omega_{\perp} = 2\pi \times 600s^{-1}$; the longitudinal frequency and the standing wave have been kept unchanged. The tunneling frequencies and probabilities $P(m)$ are given in Figs. 4(b) and 6(b), respectively. We notice that here the loss rate is much smaller, and hence the frequency shift is smaller, whereas the tunneling frequencies are slightly larger. A further reduction of the threshold value should improve the situation.

V. CONCLUSION

We have solved numerically the Gross-Pitaevskii equation for a 7Li condensate in a double-well potential and we have shown that the spatial density undergoes a symmetry breaking for a suitable number of condensed atoms. The classical asymmetrical wave function is used to select two modes. With their quantization we have evaluated the tunneling rate for some parameters of the system and we have found that it is within the reach of

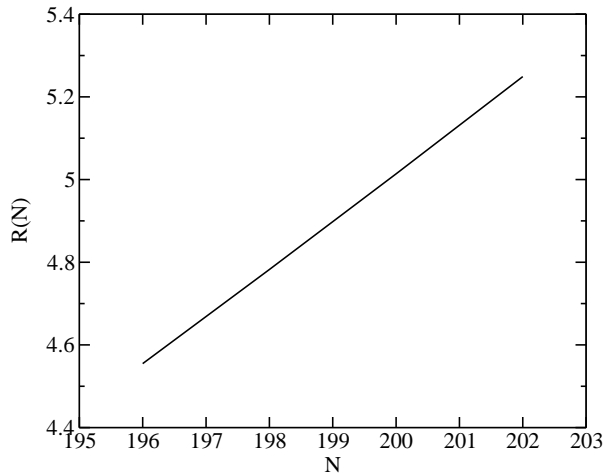


FIG. 11: $R(N)$ for the parameters of Fig. 4.

present laboratory technologies. Thermal effects could be lower than expected because of a decoupling between the collective variables and the thermal bath. To prove the presence of two alternatives we have introduced an appropriate observable. We have then evaluated the effects of loss and we have showed that the decoherence is negligible. In a forthcoming work we discuss the conditions for bistability in the case of mutual repulsion (positive scattering length).

-
- [1] M. H. Anderson et al., *Science* **269**, 198 (1995).
 [2] K. B. Davis et al., *Phys. Rev. Lett.* **75**, 3969 (1995).
 [3] C. C. Bradley et al., *Phys. Rev. Lett.* **75**, 1687 (1995).
 [4] C. C. Bradley, C. A. Sackett, and R. G. Hulet, *Phys. Rev. Lett.* **78**, 985 (1997).
 [5] R. Walsworth and L. You, *Phys. Rev. A* **56**, 555 (1997).
 [6] In the case of positive scattering length as for ^{87}Rb [1] or ^{23}Na [2], the number of atoms in a condensate may be as large as 10^6 or 10^7 , respectively.
 [7] C. Monroe et al., *Science* **272**, 1131 (1996).
 [8] M. Brune et al., *Phys. Rev. Lett.* **77**, 4887 (1996).
 [9] M. Ueda and A. J. Leggett, *Phys. Rev. Lett.* **80**, 1576 (1998).
 [10] L. Salasnich, *Phys. Rev. A* **61**, 015601 (1999).
 [11] Tin-Lun Ho, and C. V. Ciobanu, cond-mat/0011095.
 [12] In a previous report, "A. Montina and F. T. Arecchi, *J. Mod. Opt.*, **49**, 319 (2002)", we had considered this problem but in less detail; furthermore, we did not consider the role of losses on the observability of MQC.
 [13] J. I. Cirac et al., *Phys. Rev. A* **57**, 1208 (1998).
 [14] D. Gordon and C. M. Savage, *Phys. Rev. A* **59**, 4623 (1999).
 [15] D. Gordon and C. M. Savage, *Phys. Rev. A* **58**, 1440 (1998).
 [16] A generic two mode model is also used by C. Menotti et al., *Phys. Rev. A* **63**, 023601 (2001), however, here we have selected the suitable modes by reference to the associated GP equation.
 [17] R. J. Dodd et al., *Phys. Rev. A* **54**, 661 (1996).
 [18] A. J. Moerdijk et al., *Phys. Rev. A* **53**, 916 (1996).